Emerg Radiol (2011) 18:313–319
DOI 10.1007/s10140-011-0964-5

ORIGINAL ARTICLE

Radiological prognostic factors in patients with pandemic H1N1 (pH1N1) infection requiring hospital admission

Inmaculada Pinilla · Milagros Martí de Gracia · Manuel Quintana-Díaz · Juan Carlos Figueira

Received: 3 April 2011 / Accepted: 16 May 2011 / Published online: 27 May 2011

Abstract The aim of this study was to determine the radiologic findings associated with admission to the intensive care unit (ICU) and the development of acute respiratory distress syndrome (ARDS) in patients with pH1N1 infection. One hundred and four patients (15–96 years) with laboratory-confirmed pH1N1 infection seen at the Emergency Department from July to December 2009 who underwent chest radiographs were studied. Radiographs were evaluated for consolidation, ground-glass opacities, interstitial patterns, distribution, and extent of findings. Eighty-seven (83.7%) of the patients were managed in the ward, and 17 (16.3%) patients eventually required admission to the ICU. All patients admitted to the ICU showed abnormalities on the initial radiograph. The presence of consolidation, multifocal, diffuse, and bilateral involvement on the initial radiograph was associated with a statistically higher risk of requiring ICU admission ($p<0.001$). There were no significant differences regarding age, sex, and presence of underlying comorbidities. Evolution to ARDS was found in eight cases that necessitated ICU care. All of them had on the initial radiograph patchy multifocal consolidations ($p<0.001$) with bilateral lesions in six cases. A higher number of lung zones involved and consolidation on the initial chest radiograph as well as a rapid progression of the radiological abnormalities were identified in patients requiring ICU admission and development of ARDS. Initial chest radiographs show acute abnormalities in all patients with severe disease. The findings of a multifocal patchy consolidation pattern with bilateral or diffuse lung involvement on admission should alert of the impending severity of disease and the risk of necessitating ICU admission

Keywords H1N1 virus · Influenza A · Chest radiography · Computed tomography · Emergency medicine · Intensive care

I. Pinilla (✉) · M. Martí de Gracia
Department of Radiology, Hospital Universitario La Paz,
Paseo Castellana, 261,
Madrid 28046, Spain
e-mail: i.pinilla@telefonica.net

M. Quintana-Díaz
Department of Emergency, Hospital Universitario La Paz,
Madrid, Spain

J. C. Figueira
Intensive Care Unit, Hospital Universitario La Paz,
Madrid, Spain

Introduction

In the spring of 2009, an outbreak of respiratory disease caused by a novel swine-origin influenza A virus was reported in Mexico [1]. This virus, known as pandemic H1N1 (pH1N1), shared molecular features with North American and European swine, avian and human influenza viruses. Pandemic H1N1 virus is extremely contagious with person-to-person transmission [2, 3]. In June 2009, the World Health Organization (WHO) raised the pandemic level to 6 lasting until August 2010 [4]. As of 1 August 2010, more than 214 countries have reported to the WHO laboratory-confirmed cases of pandemic influenza H1N1 with over 18,449 deaths [4].

Symptoms of pH1N1 infection include: fever, cough, sore throat, rhinorrhea, dyspnea, headache, myalgia, nausea, vomiting, and diarrhea. Afebrile and atypical clinical presentations have been described in some risk groups such as pregnant women and immunosuppressed

patients [5]. Most patients have a relatively mild and self-limited disease. However, pH1N1 infection may cause severe disease requiring intensive care unit (ICU) admission because of severe hypoxemia, acute respiratory distress syndrome (ARDS), and shock [1, 5]. In contrast to seasonal influenza, children and young adults, frequently with no predisposing chronic illnesses, are more affected and prone to complications [1, 5–7]. It has been reported that between 9% and 31% of hospitalized patients required admission to the ICU, where 4–46% died [5–8]. Among the sickest patients, children seem to be more often complicated by secondary bacterial infections, whereas severe disease in adults is usually caused by primary viral pneumonia and ARDS [6].

Several reports describe the initial radiographic and CT findings in patients with H1N1 infection of both mild and severe cases including interstitial markings, nodules, ground-glass opacities (GGO), and consolidations with focal, multifocal, or diffuse distribution [8–15]. There are, however, very few reports addressing predictors of illness severity in these patients [5, 16–18]. The aim of this study was to determine the radiologic findings associated with admission to the ICU and development of ARDS in patients admitted to the Emergency Department (ED) with pandemic H1N1 influenza.

Materials and methods

The study was approved by the hospital ethics committee with a waiver of informed consent due to the observational nature of the study.

Patients

The study group consisted of 104 consecutive adult patients (at our center, any patient older than 14 years is considered an adult) with acute respiratory illness and laboratory-confirmed pH1N1 infection seen at the ED of our hospital from July to December 2009 and who underwent chest radiographs. Fifty-three were male and 51 were female. The median age was 40 years (range, 15–96 years). We reviewed the medical charts and laboratory and radiologic findings.

Microbiologic studies

Specimens from nasopharyngeal swabs and/or bronchial aspirate samples were obtained in all cases. Respiratory specimens were tested with reverse transcriptase polymerase chain reaction (PCR). A positive result was obtained in all patients. In addition, other potential respiratory pathogens were ruled out in all patients with the use of a multiplex PCR assay for respiratory viral and atypical bacterial panels for the detection of influenza A and B, adenovirus, parainfluenza, respiratory syncytial virus, rhinovirus, *Mycoplasma pneumoniae*, *Legionella pneumophila*, *Chlamydias*, and *Coxiella burnetti*.

Radiological evaluation

An initial chest radiograph was obtained in all patients on admission to the Emergency Department. Follow-up chest radiographs were obtained as clinically indicated.

Posteroanterior and lateral projection radiographs were obtained using a General Electric Healthcare digital equipment. A technique of 120 kV and 2 mAs was used for the posteroanterior view and 120 kV and 9 mAs for the lateral projection. Bedside anteroposterior projection radiographs were obtained with a mobile unit using 90 kV 5 mAs and a 100-cm film-focus distance.

Two patients underwent chest CT on a 2-detector row CT scanner (Asteion, Toshiba, Tokyo, Japan) with the following parameters: 120 kV, 180 mA, 45 s after intravenous injection of 120 mL of a nonionic contrast agent (iohexol 300 mg of iodine per milliliter).

Using the descriptors defined in the Fleischner Society's Glossary of Terms [19], chest radiographs and CT scans were evaluated for: consolidation (defined as an area of increased opacity obscuring the underlying vessels), GGO (defined as an area of increased attenuation without obscuring the underlying vessels), nodules (focal round opacity less than 3 cm), reticular opacity (defined as linear opacities forming a mesh-like pattern), and peribronchial markings (prominent peribronchial markings defined as coarse linear markings from the hila into the lungs) [20]. The location of these findings was also recorded (lobar, segmental, and number of lobes affected). The extent of disease was further categorized as unilateral or bilateral, as well as focal (defined as a single focus of abnormality), multifocal (defined as more than one focus), and diffuse (defined as involving the volume of one lung). Images were also assessed for the presence of other abnormalities such as pleural effusion and enlarged mediastinal and hilar lymph nodes. The radiological anomalies caused by underlying comorbidities or present in radiographs obtained before the acute respiratory illness were not accounted for. Radiographs and CT scans were reviewed independently by two experienced radiologists who reached a consensus decision.

Statistical analysis

All statistical analyses were carried out with the SPSS for Windows software package (Release 9.0). Quantitative data were described as the median, minimum, and maximum,

Table 1 Clinical features of 17 patients admitted to the intensive care unit

Patient no.	Age	Sex	Comorbidities	Major presenting symptom	ARDS	Other complications
1	17	F	Asthma	Fever	No	
2	71	M	COPD	Dyspnea	No	Aspergillosis, exitus
4	55	F	Morbid obesity, diabetes	Cough, fever	No	*Klebsiella pnemoniae*
6	23	F	None	Cough, fever	No	*Acinetobacter* pneumonia and empyema
8	36	F	None	Fever, dyspnea	No	
11	23	F	Asthma	Fever, dyspnea	No	
12	43	F	Morbid obesity, neoplasia	Fever, dyspnea	No	MOF, exitus
13	26	F	Seizure disorder	Fever	No	
67	52	M	None	Dyspnea	Yes	
93	56	F	None	Fever	Yes	
95	25	F	Pregnancy	Dyspnea	Yes	
96	32	F	Pregnancy	Fever	Yes	*Acinetobacter* superinfection; fibrosis
97	61	F	COPD	Dyspnea, fever	No	MOF, exitus
98	36	F	None	Fever	Yes	Fibrosis
99	46	F	Heart disease	Fever	Yes	
102	31	F	Asthma	Dyspnea	Yes	*Acinetobacter* superinfection; fibrosis
104	31	M	None	Dyspnea	Yes	Fibrosis

ARDS acute respiratory distress syndrome, *COPD* chronic obstructive pulmonary disease, *MOF* multiorgan systemic failure

while the qualitative data were represented as counts and percentages. Qualitative data were compared with Chi-square tests and quantitative variables with Mann–Whitney *U* test. Two-sided tests were used, and a p value less than 0.05 was considered statistically significant.

Results

Eighty-seven (83.7%) out of the 104 patients admitted to the ED were managed in the ward. Forty patients were female and 47 were male, ranging from 15 to 96 years with a mean age of 40 years. Forty-three of these patients had at least one coexisting medical condition that included: heart disease (n=9), asthma (n=11), chronic obstructive pulmonary disease (COPD) (n=12), immunosuppression (n=8), neurologic disease (n=1), obesity (n=1), Crohn's disease (n=1), and sickle cell disease (n=1). In 72 (82.8%) patients, posteroanterior and lateral views were obtained, and in 15 (17.2%) patients, anteroposterior projection was performed. The initial chest radiograph showed abnormalities in 34 (39.1%) patients including: consolidation in 27 (79.4%), GGO in 2 (6%), and prominent peribronchovascular markings in 7 (20.6%) cases. Lung involvement was focal in 18 (53%), multifocal in 15 (44%), and diffuse in 1 (3%) patient. The right upper lobe was involved in 8 patients, the middle lobe in 11, the left upper lobe in 10, the right lower lobe in 15, and the left lower lobe in 19 patients.

Seventeen (16.3%) out of the 104 patients admitted to the ED eventually required admission to the ICU, and 13 (76.5%) required advanced mechanical ventilation. Eleven were female and three were male, ranging in age from 17 to 71 years with a mean age of 38 years. The clinical features of the patients admitted to the ICU are summarized in Table 1. Eleven of these patients had at least one coexisting medical condition that included: asthma (n=3), COPD (n=2), morbid obesity (n=2), pregnancy (n=2), diabetes (n=1), neoplasia (n=1), seizure disorder (n=1), and heart disease (n=1). Anteroposterior chest radiograph was performed in

Fig. 1 A 52-year-old previously healthy man with influenza A infection requiring ICU admission. Anteroposterior chest radiograph at admission shows patchy small consolidations and ground-glass opacities

Table 2 Comparison between variables of patients admitted to ICU and non-admitted to ICU

Assessed variables	Non-ICU	ICU	*P* value
N	87	17	
Age (years; mean±standard deviation)	40.7±16.9	38.1±15.5	0.554
Sex (female/male)	40/47	11/3	0.304
Presence of comorbidities	43	11	0.296
Abnormalities on initial radiograph:			
Consolidation	27	16	<0.001
Reticulonodular interstitial pattern	0	1	0.07
GGO	2	1	0.284
PPM	7	0	0.999
Focal involvement	18	2	0.690
Multifocal patchy involvement	15	11	<0.001
Diffuse lung involvement	1	4	<0.001
Bilateral lung involvement	14	12	<0.001

ICU intensive care unit, *GGO* ground-glass opacities, *PPM* prominent peribronchovascular markings

ten (58.8%) patients, and both posteroanterior and lateral projections in seven (41.2%) patients. All patients admitted to ICU showed abnormalities on the initial chest radiograph on admission to the ED: consolidation in 16 (94.2%) cases, GGO in 1 (5.9%), and reticulonodular pattern in 1 (5.9%; Fig. 1). Distribution was focal in 2 (11.8%), multifocal patchy in 11 (64.7%), and diffuse in 4 (23.5%) cases. The right upper lobe was involved in six, the middle lobe in nine, the left upper lobe in four, the right lower lobe in five, and the left lower lobe in seven patients. Pleural effusions were observed on the initial radiograph in six patients. None of the patients showed hilar or mediastinal lymph node enlargement.

The clinical course of five (29%) of the patients admitted to the ICU was complicated with pulmonary superimposed infections (Table 2): three patients developed respiratory superinfections with *Acinetobacter*, (two of them also developed ARDS), one with Klebsiella, and in one patient, pH1N1 infection was complicated with fatal secondary invasive pulmonary aspergillosis. Two patients died from shock and multiorgan systemic failure and one patient from systemic secondary infection with *Aspergillus*.

The comparison between the clinical and radiological characteristics of the patients admitted to the ICU and those managed without ICU care is shown in Table 2. The presence on the initial chest radiograph of lung consolidation, multifocal, diffuse, and bilateral involvement (Fig. 2) was associated with a statistically higher risk of requiring ICU admission ($p<0.001$). There were no significant differences between both groups regarding age, sex, and the presence of underlying comorbidities.

Evolution to ARDS was found in eight cases (6.7%) that necessitated ICU care, all of them requiring advanced mechanical ventilation. The clinical and radiological features as well as the evolution of patients with ARDS are summarized in Table 3. All of them had on the initial radiograph a patchy multifocal consolidation pattern of involvement ($p<0.001$) with bilateral lesions in six cases. CT scans were available in two of these patients. In both cases, patchy areas of parenchymal consolidation and GGO as well as small pleural effusions were found (Fig. 3). No nodules, reticular pattern, or lymphadenopathies were found. In five out of eight patients, a rapid progression of the initial radiological abnormalities in less than 48 h was

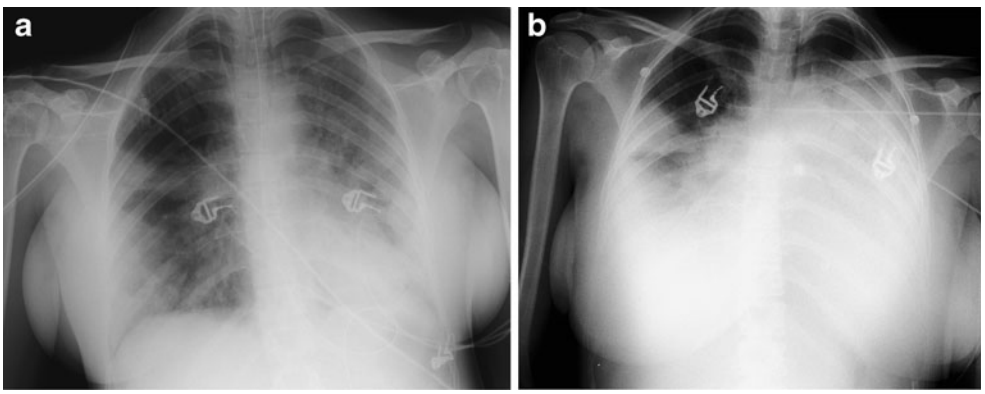

Fig. 2 A 32-year-old pregnant woman who suffered H1N1 virus infection. **a** Anteroposterior chest radiograph obtained the day of admission to the ICU shows patchy nonsymmetric bilateral consolidations. **b** The patient developed ARDS. Bedside anteroposterior plain chest film obtained at the ICU 24 h after hospital admission reveals rapid disease progression with extensive bilateral lung consolidations

Table 3 Summary of the clinical and imaging features in eight patients developing ARDS

Patient no.	Age and sex	Underlying comorbidities	No. of lobes	Radiographic pattern, distribution and evolution of anomalies		Onset of ARDS	Onset of improvement	Fibrosis
				Initial	Follow-up			
67	52/M	None	4	Patchy multifocal consolidation	Rapid progression 48H	2nd D	2nd W	No
93	56/F	None	4	Consolidations, GGO, PlE	Waxing and waning for 4W	2nd W	5th W	No
95	25/F	Pregnancy	4	Diffuse consolidation, PlE	Rapid progression 48H	1st W	2nd W	No
96	32/F	Pregnancy	2	Patchy multifocal consolidation	Rapid progression 48H	1st W	2nd W	Yes
98	36/F	None	2	Patchy multifocal consolidation	Rapid progression 48H	3rd W	6th W	Yes
99	46/F	Heart disease	3	Patchy multifocal consolidation	Waxing and waning for 3W	3rd W	6th W	No
102	31/F	Asthma	5	Diffuse consolidation, PE	Rapid progression 48H	2nd D	1st W	Yes
104	31/M	None	4	Diffuse consolidation	Progression during 2W	2nd W	3rd W	Yes

ARDS acute respiratory distress syndrome, *No. of lobes* number of lung lobes involved on chest radiograph, *GGO* ground-glass opacities, *PlE* pleural effusion, *H* hours, *D* day, *W* week

observed. Eventually, four patients developed fibrosis on follow-up thoracic imaging. In the multivariant analysis, a higher number of lung zones were involved, and the patchy consolidation pattern on the initial chest radiograph as well as a rapid progression of the radiological abnormalities within the first 48 h were identified in patients requiring ICU admission and development of ARDS.

Discussion

The 2009 pandemic H1N1 influenza A virus has rapidly spread worldwide, resulting in the first influenza pandemic in the twenty-first century [5]. The clinical spectrum of the pH1N1 infection ranges from acute mild respiratory illness to a severe viral pneumonia that may be associated with profound hypoxemia, ARDS, and sometimes shock [1, 5]. The importance of early administration of antiviral drugs in the treatment of severe cases has been highlighted [5, 6, 9]. Therefore, early identification of patients with a high risk for a complicated course may assist in patient management.

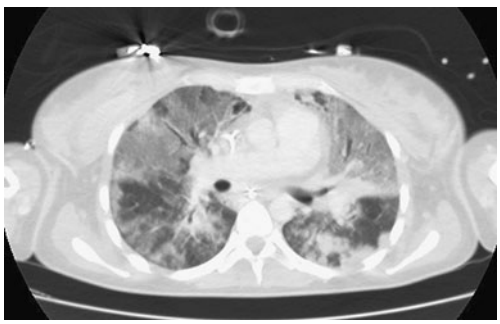

Fig. 3 A 32-year-old pregnant woman with H1N1 virus infection who developed ARDS (same patient as in Fig. 2). Chest CT (lung window) reveals widespread ground-glass opacities and small perihilar and peripheral foci of parenchymal consolidation in lower lobes

Zimmerman et al. [5] found that the elevated C-reactive protein level on admission to the ED significantly correlated with impending disease severity in patients infected with pH1N1 [6]. Also, coinfection with *Streptococcus pneumoniae* has been correlated with illness severity [17]. However, studies assessing radiological findings at presentation that might be used as predictors of the severity of disease are sparse [8, 18].

Our results show that the initial chest radiograph on admission to the ED is invariably abnormal in patients with pH1N1 infection that eventually require mechanical ventilation and ICU admission. In contrast, more than half of patients with mild self-limited disease show a normal initial radiograph. These findings are in concordance with those of other studies carried out in both pediatric [10] and in adult populations [8, 11], reporting between 45% and 67% of normal initial radiographs. However, Aviram et al. [18] reported normal initial radiographs in 3% of patients requiring mechanical ventilation.

In our series, the most frequent radiological abnormality in patients with pH1N1 infection was lung consolidation, similar to the reported data for pH1N1 virus as well as for other influenza virus [3, 20–23]. We have found a slightly lower lobe predominance of the abnormalities, an inconstant finding in the literature. As Lee et al. [10], we found

prominent peribronchial marking in a substantial minority in the subgroup of patients that did not precise ICU admission. This pattern, which is rare on other series of adult patients with pH1N1 infection, may be explained by the inclusion of very young patients, between 14 and 20 years in our cohort. It has been attributed to age-related differences in immunity [10].

In our study, the most common radiological pattern on admission to the ED in patients eventually requiring intensive care measures was bilateral multifocal patchy consolidation. Diffuse lung involvement was found in 25% of these patients. These findings are consistent with those inferred from the literature in the subgroups of sickest patients [8–13, 18]. In the largest series, Aviram et al. [18] reported that extensive lung involvement as expressed by multizonal and bilateral peripheral opacities on the initial radiograph was associated with adverse prognosis. One difference is, however, the lower prevalence of GGO in our series compared with other reports in which there were a higher number of patients studied with CT. In addition, the fact that a substantial proportion of bedside anteroposterior radiographs (instead of the two projections) were obtained in the group of patients with eventual admission to ICU may have decreased the detection of subtle areas of GGO and underestimated the presence of small consolidations in the retrocardiac area.

In our study, most patients developing ARDS showed progression of the radiological abnormalities (multifocal areas of lung consolidation) within 48 h of admission to the ED. The rapid progression of viral pneumonia caused by pH1N1 leading to intubation within 24 h of diagnosis has been previously reported [5].

As Aviram et al. [18], we have not observed a significant association between the presence of comorbidities and a complicated course of the infection with ICU admission. This is in high contrast with the findings reported by Lee et al. [10], although their study was carried out in patients under 20 years of age, and it has been communicated that severe cases among pediatric patients occur predominantly in children with underlying conditions, while adults seem to have severe viral pneumonia and ARDS often in previously healthy subjects [6].

Our study has several limitations. Firstly, it is retrospective in nature, and it includes a limited number of patients necessitating mechanical ventilation and intensive care measures. In addition, it is difficult to draw conclusions about the actual prevalence of abnormal chest radiographs and the evolution to severe viral pneumonia because an undetermined number of patients with a mild form of illness may have not sought attention at the hospital ED or their physicians may have different criteria to perform thoracic imaging. Secondly, correlation with CT, which is more accurate, was available only in two patients. This fact may account for the lower prevalence of GGO in our series compared with the literature. However, it must be noted that CT does not play a significant role in the initial diagnosis of pH1N1 infection, and it should not be used in the initial evaluation, especially in children. Thirdly, none of our patients underwent lung biopsy for histopathologic correlation.

In conclusion, initial chest radiographs show acute abnormalities in all patients with severe disease. The findings of a multifocal patchy consolidation pattern with bilateral or diffuse lung involvement on admission should alert of the impending severity of disease and the risk of necessitating ICU admission.

References

1. Pérez-Padilla R, de la Rosa-Zamboni D et al (2009) Pneumonia and respiratory failure from swine-origin influenza A (H1N1) in Mexico. N Engl J Med 361:680–9
2. Centers for Disease Control and Prevention (2009) Swine influenza A (H1N1) infection in two children—Southern California, March–April 2009. MMWR Morb Mortal Wkly Rep 58:400–2
3. Dawood FS, Jain S, Finelli L, Virus Investigation Team et al (2009) Emergence of a novel swine-origin influenza A (H1N1) virus in humans. N Engl J Med 360:2605–15
4. World Health Organization Website. Global alert and response: current WHO phase of pandemic alert. http://www.who.int/csr/disease/avian_influenza/phase/en/index.html. Accessed 19 Mar 2011
5. Writing Committee of the WHO Consultation on Clinical Aspects of Pandemic (H1N1) 2009 Influenza (2010) Clinical aspects of pandemic 2009 influenza A (H1N1) virus infection. N Engl J Med 362:1708–19
6. Rothberg MB, Haessler SD (2010) Complications of seasonal and pandemic influenza. Crit Care Med 38(suppl):e91–e-97
7. Domínguez-Cherit G, Lapinsky SE, Macias AE et al (2009) Critically ill patients with 2009 influenza A (H1N1) in Mexico. JAMA 302:1880–7
8. Abbo L, Quartin A, Morris MI et al (2010) Pulmonary imaging of pandemic influenza H1N1 infection: relationship between clinical presentation and disease burden on chest radiography and CT. Br J Radiol 83:645–51
9. Yun TJ, Kwon GJ, Oh MK et al (2010) Radiological and clinical characteristics of a military outbreak of pandemic H1N1 2009 influenza virus infection. Korean J Radiol 11:417–24
10. Lee EY, McAdam AJ, Chaudry G, Fishman MP, Zurakowski D, Boiselle PM (2010) Swine-origin influenza A (H1N1) viral infection in children: initial chest radiographic findings. Radiology 254:934–41
11. Agarwall PP, Cinti S, Kazerooni EA (2009) Chest radiographic and CT findings in novel swine-origin influenza A (H1N1) virus (S-OIV) infection. AJR 193:1488–93
12. Ajlan AM, Quiney B, Nicolaou S, Müller NL (2009) Swine-origin influenza A (H1N1) viral infection: radiographic and CT findings. AJR 193:1494–9
13. Marchiori E, Zanetti G, Hochhegger B et al (2010) High-resolution computed tomography findings from adult patients with influenza A (H1N1) virus-associated pneumonia. Eur J Radiol 74:93–8
14. Theodorou DJ, Theodorou SJ, Tsoumani A et al (2010) Radiographic and CT findings in pandemic swine-origin influenza A (H1N1). Eur J Intern Med 21(2):e7–8

15. Martí de Gracia M, Pinilla I, Quintana-Díaz M et al (2011) Gripe A, ¿diferente de la gripe estacional? Radiología 53:159–65
16. Zimmerman O, Rogowski O, Aviram G et al (2010) C-reactive protein serum levels as an early predictor of outcome in patients with pandemic H1N1 influenza A virus infection. BMC Infect Dis 10:288–95
17. Palacios G, Hornig M, Cisterna D et al (2009) *Streptococcus pneumoniae* coinfection is correlated with the severity of H1N1 pandemic influenza. PLoS ONE 4:e8540
18. Aviram G, Bar-Shali A, Sosna J et al (2010) H1N1 influenza: chest radiographic findings in helping predict patient outcome. Radiology 255:252–9
19. Hansell DM, Bankier AA, MacMahon H et al (2008) Fleischner Society: glossary of terms for thoracic imaging. Radiology 246:697–722
20. Donnelly LF (2005) Chest. In: Donnelly LF (ed) Diagnostic imaging: pediatrics. Amirsys, Salt Lake City, pp 62–74
21. Kim EA, Lee KS, Primack SL et al (2002) Viral pneumonias in adults: radiologic and pathologic findings. Radiographics 22:S137–49
22. Oikonomou A, Müller NL, Nantel S (2003) Radiographics and high-resolution CT findings of influenza virus pneuomonia in patients with hematologic malignancies. AJR Am J Roentogenol 181:507–11
23. Qureshi NR, Hien TT, Farrar J et al (2006) The radiologic manifestations of H5N1 avian influenza. J Thorac Imaging 21:259–64